Monthly Notices
of the
ROYAL ASTRONOMICAL SOCIETY

MNRAS **493,** 4308–4314 (2020)
Advance Access publication 2020 February 21

doi:10.1093/mnras/staa519

Evidence of an evolved nature of MWC 349A

M. Kraus ,[1]★ M. L. Arias,[2,3]★† L. S. Cidale[2,3]★† and A. F. Torres[2,3]†

[1]*Astronomical Institute, Czech Academy of Sciences, Fričova 298, 251 65 Ondřejov, Czech Republic*
[2]*Departamento de Espectroscopía Estelar, Facultad de Ciencias Astronómicas y Geofísicas, Universidad Nacional de La Plata, Paseo del Bosque S/N, La Plata, B1900FWA, Buenos Aires, Argentina*
[3]*Instituto de Astrofísica de La Plata, CCT La Plata, CONICET-UNLP, Paseo del Bosque S/N, La Plata, B1900FWA, Buenos Aires, Argentina*

Accepted 2020 February 18. Received 2020 February 18; in original form 2019 December 19

ABSTRACT

The Galactic emission-line object MWC 349A is one of the brightest radio stars in the sky. The central object is embedded in an almost edge-on oriented Keplerian rotating thick disc that seems to drive a rotating bipolar wind. The dense disc is also the site of hot molecular emission such as the CO bands with its prominent band heads in the near-infrared spectral range. Despite numerous studies, the nature of MWC 349A is still controversial with classifications ranging from a pre-main sequence object to an evolved supergiant. We collected new high-resolution near-infrared spectra in the *K* and *L* bands using the GNIRS spectrograph at Gemini-North to study the molecular disc of MWC 349A, and in particular to search for other molecular species such as SiO and the isotope ^{13}CO. The amount of ^{13}CO, obtained from the ^{12}CO/^{13}CO ratio, is recognized as an excellent tool to discriminate between pre-main-sequence and evolved massive stars. We find no signatures of SiO band emission, but detect CO band emission with considerably lower intensity and CO gas temperature compared to previous observations. Moreover, from detailed modelling of the emission spectrum, we derive an isotope ratio of $^{12}\mathrm{CO}/^{13}\mathrm{CO} = 4 \pm 1$. Based on this significant enrichment of the circumstellar environment in ^{13}CO, we conclude that MWC 349A belongs to the group of B[e] supergiants, and we discuss possible reasons for the drop in CO intensity.

Key words: stars: massive – stars: emission line, Be – circumstellar matter – stars: individual: MWC 349A.

1 INTRODUCTION

The emission-line object MWC 349A ($\alpha = 20^{\mathrm{h}}32^{\mathrm{m}}45\overset{\mathrm{s}}{.}53$, $\delta = 40^{\circ}39'36\overset{''}{.}60$) is one of the brightest radio stars in the sky (Braes, Habing & Schoenmaker 1972). Radio continuum observations suggest that MWC 349A is driving an ionised wind with an outflow velocity of 25–50 km s^{-1} (Altenhoff, Strittmatter & Wendker 1981) and a mass-loss rate of 10^{-5} M$_{\odot}$ yr^{-1} (Olnon 1975). The lack of photospheric absorption lines hampers significantly the assignment of a proper classification, but the numerous He I lines in emission speak in favour of a hot central source with a spectral type between late O (Hartmann, Jaffe & Huchra 1980) and about B0 (Hofmann et al. 2002). Estimates for the object's distance and luminosity range from 1.2 (Cohen et al. 1985) to 1.7 kpc (Meyer, Nordsieck & Hoffman 2002), and from 3×10^4 L$_{\odot}$ (Cohen et al. 1985) to 8×10^5 L$_{\odot}$ (Gvaramadze & Menten 2012), respectively. This distance range is consistent with the parallax and its error provided by *Gaia* DR2 (Gaia Collaboration et al. 2018). The central object suffers from an extinction of $A_V \simeq 10$ mag, of which about two magnitudes seem to be circumstellar in origin (Cohen et al. 1985).

The morphology of the radio emission at 6 cm is spherical (Cohen et al. 1985), whereas at 2 cm it reveals a bipolar shape of the ionized wind with an east-west extent smaller than 0.4 arcsec, indicating an equatorial disc seen edge-on (White & Becker 1985). The star has a strong infrared (IR) excess emission (Geisel 1970), indicating large amounts of circumstellar dust, and a dusty disc oriented in east-west direction was resolved by infrared interferometric (Danchi, Tuthill & Monnier 2001) as well as by speckle interferometric observations (Mariotti et al. 1983; Leinert 1986). IR images at 24 μm taken with the *Spitzer Space Telescope* show an extended (over several arcminutes) infrared double-cone (or X-shaped nebula) structure (Gvaramadze & Menten 2012; Strelnitski et al. 2013). Moreover, many optical and IR emission lines of elements in diverse ionization states display double-peaked profiles (Andrillat, Jaschek & Jaschek 1996; Aret, Kraus & Šlechta 2016). These have been suggested to form within a Keplerian rotating neutral gas disc with an ionized surface layer (e.g. Hamann & Simon 1986).

★ E-mail: michaela.kraus@asu.cas.cz (MK);
mlaura@fcaglp.fcaglp.unlp.edu.ar (MLA);
lydia@fcaglp.fcaglp.unlp.edu.ar (LSC)
† Member of the Carrera del Investigador Científico, CONICET

Additional support for a rotating circumstellar disc is provided by the numerous hydrogen recombination maser and laser lines for which MWC 349A is famous. The first maser lines at mm wavelengths have been discovered by Martin-Pintado et al. (1989), and since then, many more maser and laser transitions have been identified that spread from the far-infrared up to the millimetre range (Thum et al. 1994a, b, 1998; Strelnitski et al. 1996). Modelling of the maser lines reveals that their profiles consist of two components: one in agreement with Keplerian rotation within a narrow circumstellar ring and another one suggesting a wind emanating from and co-rotating with the disc (e.g. Martín-Pintado et al. 2011; Báez-Rubio et al. 2013, 2014; Báez-Rubio & Martín-Pintado 2017; Zhang et al. 2017).

MWC 349 has been proposed to be a binary system, in which the companion, a B0 III star (MWC 349B), is located about 2.4 arcsec west of the massive and luminous B[e] component MWC 349A (White & Becker 1985). However, recent analysis of the radial velocities of the two objects seems to speak against a gravitationally bound system, which reopens the discussion whether MWC 349A belongs to the Cygnus OB2 association (Drew et al. 2017).

Despite numerous studies about MWC 349A, the nature of this enigmatic object remains elusive. Classifications range from a massive pre-main-sequence object due to the disc-bipolar wind shape seen on small scales on radio images and traced by the maser and laser lines (e.g. Cohen et al. 1985; Strelnitski et al. 2013) to an evolved massive star such as a B[e] supergiant (Hartmann et al. 1980, 2002) or a luminous blue variable (Gvaramadze & Menten 2012) based on the huge, up to 5 pc scale infrared nebula structure associated with the star. To solve the issue of the unclear evolutionary state of MWC 349A, once and for all, a trustworthy age indicator is needed.

As was shown by Kraus (2009), the most ideal tool to discriminate between a young, pre-main sequence and an evolved nature of a massive star is provided by the abundance ratio between ^{12}C and its isotope ^{13}C measured in terms of the molecular abundance ratio ^{12}CO/^{13}CO within their circumstellar environments. In the pre-main-sequence stage, the ^{12}C/^{13}C ratio has the interstellar value of ∼90 (see e.g. Ekström et al. 2012). During the evolution of a massive star, the surface abundance ratio changes considerably, and the value can drop to ^{12}C/^{13}C < 10 or even ^{12}C/^{13}C < 5, depending on the initial mass of the star and its rotation that mixes chemically processed material to the surface. Once on the surface, the isotopes are transported via mass-loss in form of stellar winds and mass ejections to the environment. There, they can be bound in ^{12}CO and ^{13}CO, in case the physical parameters in the environment, in terms of density and temperature favour the condensation of molecules.

Circumstellar discs provide the most ideal environments in which molecules can form and survive in substantial amounts. Within the discs, the molecules are shielded from the dissociating stellar ultraviolet radiation field. Emission from hot CO gas has been detected in the IR spectra of both accretion discs of pre-main-sequence stars (e.g. Geballe & Persson 1987; Carr 1989, 1995; Wheelwright et al. 2010; Ilee et al. 2013, 2018) and discs formed from the outflows and ejecta of evolved massive stars such as the B[e] supergiants (McGregor, Hyland & Hillier 1988a; McGregor, Hillier & Hyland 1988b; McGregor, Hyland & McGinn 1989; Morris et al. 1996; Wheelwright et al. 2012; Kraus et al. 2016, 2017; Kourniotis et al. 2018; Maravelias et al. 2018; Torres et al. 2018). Enrichment in ^{13}CO has been found, based on measurements of the ^{12}CO/^{13}CO ratio in high-quality near-IR spectra, solely in the discs of confirmed evolved objects (Liermann et al. 2010; Oksala et al. 2013; Kraus et al. 2013b, 2014), reinforcing the power of this isotope-ratio method for the discrimination between young and evolved stars (Muratore et al. 2015).

CO band emission from MWC 349A was discovered by Geballe & Persson (1987). Although their spectral range covered the positions of the first ^{13}CO band head, the identification of the isotope was uncertain due to the very low resolution ($R \sim 650$) of their spectra. Follow-up observations in the *K*-band had either similarly low resolution, or were limited to studies of the first band heads of ^{12}CO to determine the kinematics within the molecular emission region (Kraus et al. 2000).

In this work, we wish to solve the long-standing issue of the unclear nature of MWC 349A. For an unambiguous classification as either a pre-main-sequence object or an evolved massive star, we acquired new high-quality near-IR spectra, which allow us to measure precisely the ^{12}CO/^{13}CO ratio in its circumstellar disc. Moreover, we aim to search for emission from SiO. The detection of emission from hot SiO gas would allow us to derive complementary information about the physical properties within the molecular disc of MWC 349A (see Kraus et al. 2015).

2 OBSERVATIONS AND REDUCTION

A medium-resolution ($R \sim 6\,000$) *K*-band spectrum was acquired on 2013 July 7 and high-resolution ($R \sim 18\,000$) *K*- and *L*-band spectra on 2013 August 18. The observations were carried out using the Gemini Near-InfraRed Spectrograph (GNIRS; Elias et al. 2006) at GEMINI-North under Program IDs GN-2013A-Q-78 and GN-2013B-Q-11. For each science acquisition, a telluric standard star was observed close in time and airmass.

The medium-resolution spectrum was taken with the 110.51 mm^{-1} grating, the short camera, and the 0.″3 slit. It covers the wavelength range from 2.280 to 2.475 μm.

The high-resolution spectra were taken with the 110.51 mm^{-1} grating, the long camera (0.05 arcsec pix^{-1}) and the 0.1 arcsec slit. In the *K* band, the spectra were centred on 2.312 and 2.36 μm to trace the molecular emission of the CO isotopes ^{12}CO and ^{13}CO, and in the *L* band on 4.05 μm to cover the region of the SiO bands.

Exposures for the target and the telluric standard star were taken in two positions along the slit (A and B) with a series of ABBA sequences. Data reduction was performed with standard IRAF[1] tasks. The procedure includes subtraction of AB pairs, flat-fielding, and telluric correction. The wavelength calibration was performed using the telluric lines. The high-resolution *K*- and *L*-band spectra achieved signal-to-noise ratios of ∼130 and ∼280, respectively. The final spectra were normalized to the continuum.

The medium- and high-resolution *K*-band spectra, taken with a separation of about one month, show no noticeable difference in the appearance of the emission features. Therefore, the following investigation and analysis is based purely on the high-resolution spectrum.

3 RESULTS

Figs 1 and 2 show the observed high-resolution spectra of MWC 349A in the *K* and *L* bands, respectively. The *K*-band displays

[1] IRAF is distributed by the National Optical Astronomy Observatory, which is operated by the Association of Universities for Research in Astronomy (AURA) under cooperative agreement with the National Science Foundation.

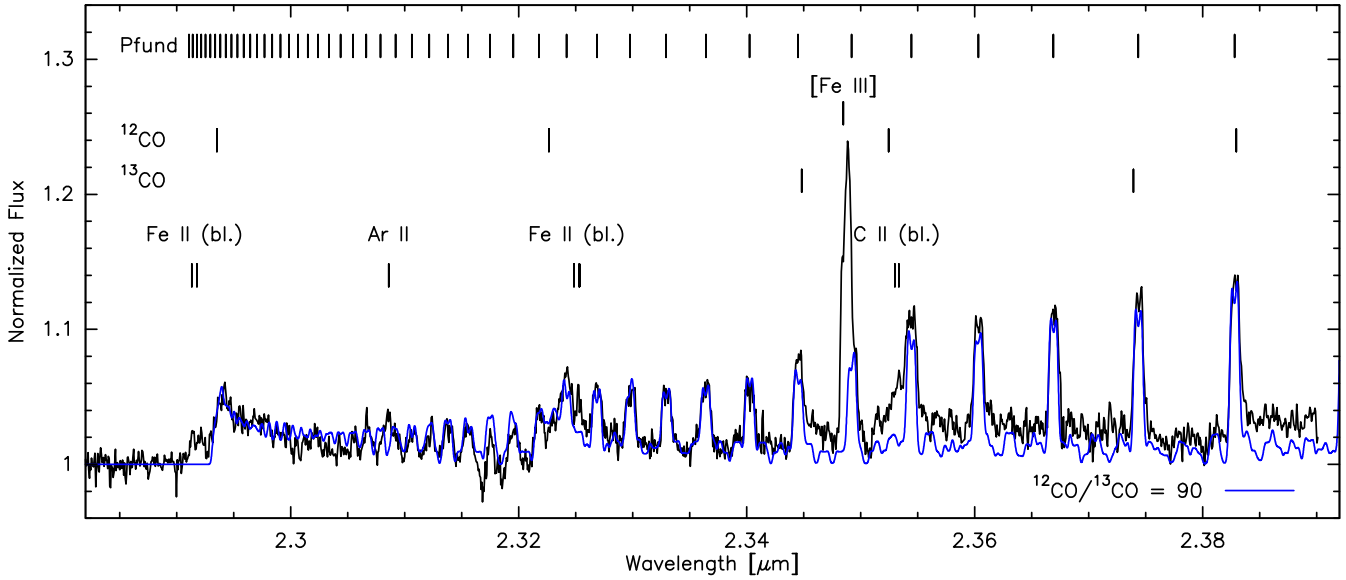

Figure 1. Normalized high-resolution *K*-band spectrum (black) of MWC 349A, showing the most prominent emission lines and the positions of the band heads of ^{12}CO and ^{13}CO. The best-fitting model (blue) is also shown. It is the superposition of the emission from the Pfund series and the CO-band emission for an isotope abundance ratio of 90 (interstellar value). See Section 3 for details.

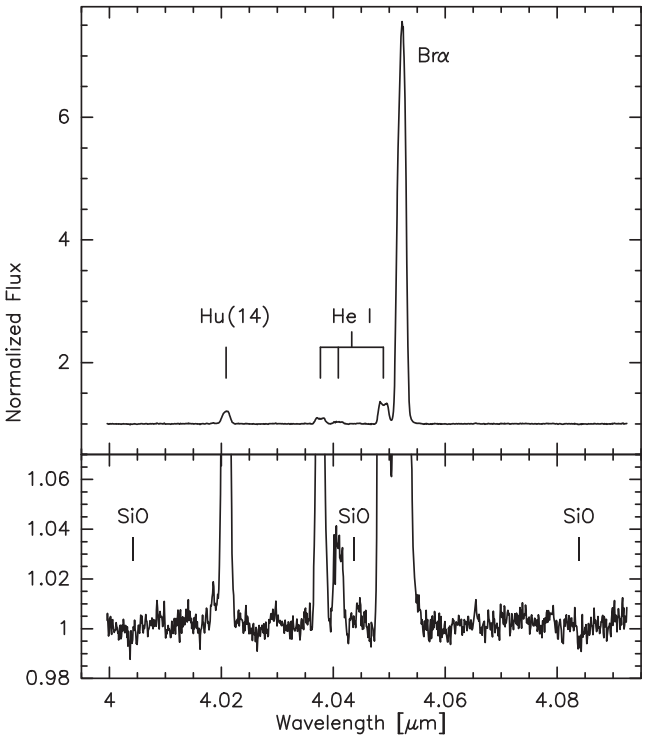

Figure 2. High-resolution *L*-band spectrum of MWC 349A with prominent emission lines labelled (top). The bottom panel is a zoom around the continuum, indicating the wavelengths of the SiO band heads.

emission lines from the Pfund series ranging from Pf (24) up to Pf (62), weak CO band emission, as well as emission from a few metallic lines. Their wavelengths and identifications are given in columns 1 and 2 of Table 1, respectively. The line identification is based on wavelengths retrieved from the NIST Atomic Spectra Database,[2] except for the line [Fe III] λ2.3485 that was taken from Lumsden & Puxley (1996). The wavelengths of the CO band heads were taken from Kraus et al. (2000).

Table 1. Identification of emission lines besides the lines Pf (24) to Pf (62) of the Pfund series.

K band		*L* band	
λ (μm)	Element	λ (μm)	Element
2.2913	Fe II	4.0209	Hu (14)
2.2918	Fe II	4.0377	He I
2.2935	^{12}CO (2–0)	4.0409	He I
2.3086	Ar II	4.0490	He I
2.3227	^{12}CO (3–1)	4.0522	Br α
2.3248	Fe II	–	–
2.3253	Fe II	–	–
2.3448	^{13}CO (2–0)	–	–
2.3485	[Fe III]	–	–
2.3525	^{12}CO (4–2)	–	–
2.3530	C II	–	–
2.3533	C II	–	–
2.3739	^{13}CO (3–1)	–	–

The only lines we could identify in the *L* band are from hydrogen and He I (see columns 3 and 4 of Table 1). No traces of emission from the SiO molecule are found (see the bottom panel of Fig. 2). First-overtone band emission of SiO has been detected so far from the high-density environments of four B[e] stars (Kraus et al. 2015), and in all four cases, the intensity in the SiO bands was 5–15 times lower than the intensity in the first-overtone CO bands published by Maravelias et al. (2018). Considering that such a trend might also apply to MWC 349A, the weakness of its CO band emission with only ∼5–6 per cent of the continuum flux might be the reason for the absence of detectable SiO-band emission.

[2]https://www.nist.gov/pml/atomic-spectra-database (Kramida et al. 2019)

3.1 Pfund line emission

The high-resolution *K*-band spectrum (Fig. 1) shows that the Pfund lines display slightly double-peaked profiles, implying rotational motion of the ionized gas. To model the Pfund line emission, we utilize the code developed by Kraus et al. (2000) that computes the emission of the series according to Menzel case B recombination, assuming that the lines are optically thin.

For the computations of the line intensities, we fix the electron temperature at 10 000 K, which is a suitable value for the ionized gas around a hot OB-type star. Fixing the temperature has no significant impact on the shape of the lines or the relative line intensities of the individual Pfund lines. The observed *K*-band spectrum implies a cut-off in the Pfund series indicating pressure ionization. The maximum number of the series, Pf(62), delivers a hydrogen density of $(3.5 \pm 0.3) \times 10^{12}$ cm^{-3} within the line-forming region. Considering a partially ionized gas, this value poses an upper limit for the electron density. We use this value for the computation of the Pfund line spectrum. For such a high density, the emission is in local thermodynamic equilibrium (LTE).

For the profile function, we assume that the emission of the Pfund lines emerges from a narrow ring of gas with constant temperature and density revolving the star. This assumption is justified based on the double-peaked profiles that we observe for the Pfund lines. The inclination angle of the system is fixed at 80° under the convention that an edge-on orientation corresponds to an inclination angle of 90°. This choice of 80° has been made to be in line with the model considerations for the CO band emission (see below). Then, the only free parameters for the computation of the Pfund line emission spectrum are the rotation velocity, $v_{\rm rot,\,Pf}$, and a Gaussian component $v_{\rm gauss,\,Pf}$. This Gaussian component combines the broadening contributions from a possible turbulent motion of the gas (or a possible wind component) and the contribution of the thermal motion. The final Pfund emission spectrum is convolved with the resolution of the spectrograph.

We obtain reasonable fits to the observed line profiles for a rotation velocity of 45 ± 5 km s^{-1} in combination with a Gaussian component of 20 ± 5 km s^{-1}. This high value for the Gaussian velocity is needed to reproduce the line wings and the shallowness of the double peak structure. Considering a contribution of 12–13 km s^{-1} for the thermal motion, we derive a turbulent component of about 15 ± 5 km s^{-1}.

3.2 CO band emission

Our spectrum spreads over a wide wavelength range, covering the positions of the first four band heads of ^{12}CO and the first two band heads of ^{13}CO (Fig. 1). However, due to the strong contamination with the Pfund emission lines, only the first two band heads of ^{12}CO can be easily identified by eye in the spectrum.

For the computation of the molecular bands, we use the code developed by Kraus et al. (2000) for ^{12}CO emission from a rotating disc, which was advanced by Kraus (2009) and Oksala et al. (2013) to include the bands of the isotope ^{13}CO. The calculations are performed under the assumption of LTE which is a suitable approach for dense gas discs. The wide structure of the first band head of ^{12}CO indicates kinematic broadening, although no clear hints for a blue shoulder and a red peak of the band head is obvious, as is typically the case for CO band emission from a rotating disc (see e.g. Carr 1995; Kraus et al. 2000, 2013b, 2016; Muratore et al. 2015; Maravelias et al. 2018). Therefore, we follow the approach of Kraus et al. (2000), who proposed that the CO emission of

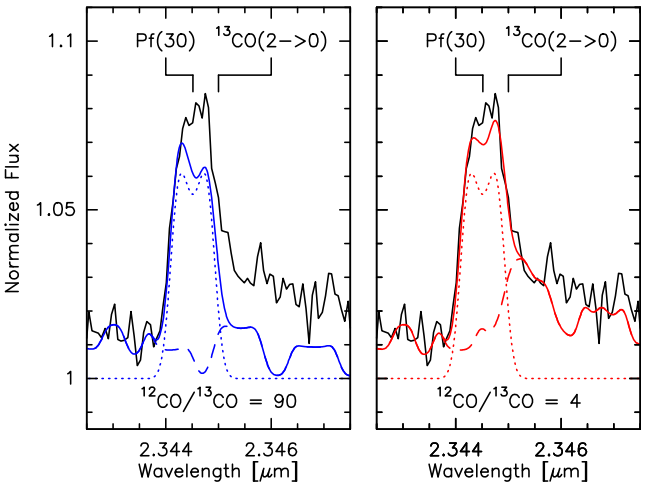

Figure 3. Model fits (colour) to the observations (black) zoomed to the region around the Pf(30) line. The dashed and dotted lines represent the pure CO and pure Pfund contribution to the combined fit (solid line). The fits in the left and right panels correspond to models with ^{12}CO/^{13}CO isotope ratios of 90 and 4, respectively.

MWC 349A originates from the far side of the inner rim of the almost edge-on ($i = 80°$) Keplerian disc, meaning that we compute the profiles of each individual CO ro-vibrational line for a symmetric ring segment with a velocity range spreading from −59 to +59 km s^{-1}.

To fix the physical parameters of the CO emitting region, we first focus on the short-wavelength part of the spectrum ($\lambda < 2.34$ μm) that covers only the first two band heads of ^{12}CO. In this wavelength region no contribution from ^{13}CO arises. To reduce the number of free parameters, we assume a constant temperature and column density for the molecular gas. We compute a grid of models for the CO parameters, convolve the synthetic CO spectra with the resolution of the spectrograph, combine the Pfund with the CO emission spectra and fit these total theoretical spectra to the observations. From visual inspection of the fits, the best-fitting model is found for a gas temperature of $T_{\rm CO} = 1500 \pm 200$ K and a ^{12}CO column density of $N_{\rm CO} = (1.0 \pm 0.5) \times 10^{21}$ cm^{-2}.

Then we include ^{13}CO into the model. As we do not know the ^{12}CO/^{13}CO ratio a priori, we start from the interstellar value, which is ∼90. Note, that such a small ^{13}CO contribution remains basically undetectable in the total spectrum, because the intensity scales approximately with the column density of the gas. The fit of the combined ^{12}CO, ^{13}CO, and Pfund emission to the observed spectrum is shown as the blue line in Fig. 1.

From inspection of the fit we note that the model underestimates the observed intensity in the long-wavelength region ($\lambda > 2.344$ μm). This underestimation is particularly noticeable in the red peak and wing of the Pfund line Pf(30) at 2.3445 μm (see the left-hand panel of Fig. 3). At this wavelength, the only known spectral feature[3] is the first band head of ^{13}CO. The disagreement between model and observations indicates that a significant amount of ^{13}CO is present in the spectrum. The best-fitting model is obtained for

[3]We wish to emphasize that this feature cannot be a telluric remnant. Telluric lines spread over the full range of the CO bands. Improper correction for the telluric pollution would result in remnants all over the spectrum, which are not seen. In addition, the band head of ^{13}CO is a very broad emission feature in contrast to the sharp telluric lines.

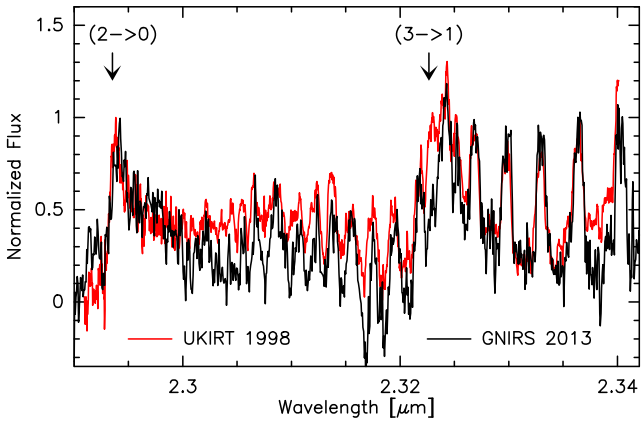

Figure 4. UKIRT spectrum taken in 1998 (red) superimposed on the GNIRS spectrum taken in 2013 (black). Marked are the positions of the ^{12}CO band heads (2 ⟶ 0) and (3 ⟶ 1). For easier comparison, the emission is normalized to the intensity of the first band head.

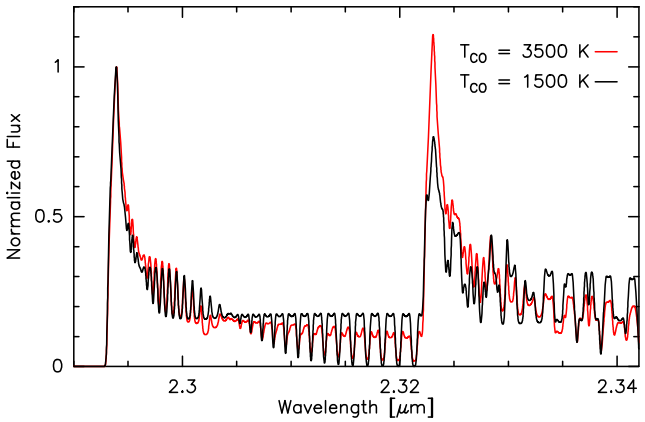

Figure 5. Model spectra of pure ^{12}CO band emission calculated for the two indicated temperature values. For easier comparison, the emission is normalized to the intensity of the first band head.

an isotope ratio of ^{12}CO/^{13}CO = 4 ± 1. This result is shown in red in the right-hand panel of Fig. 3. Such a high contribution of ^{13}CO provides clear evidence for an evolved nature of MWC 349A and rules out a pre-main-sequence evolutionary state of the star.

4 DISCUSSION

We note clear differences in the physical parameters needed for the computation of the ^{12}CO band emission when comparing the results obtained from our GNIRS spectrum taken in 2013 with those derived by Kraus et al. (2000) from the spectrum taken in 1998 with the United Kingdom Infrared Telescope (UKIRT). While the ^{12}CO column density in 1998 ($N_{CO} \sim 5 \times 10^{20}$ cm^{-2}) was slightly lower but still within the errorbars of our value, the CO temperature ($T_{CO} \simeq 3500$ K) was more than twice higher in 1998 compared to the low value of $T_{CO} \simeq 1500$ K we found now. Because of the similar resolution of the UKIRT ($R \sim 20\,000$) and the GNIRS spectra ($R \sim 18\,000$), this discrepancy in parameters points towards a change in excitation conditions within the disc of MWC 349A, which can be verified in case the two observed spectra display profound differences.

In general, the intensity of the emission in the GNIRS spectrum is lower than in the UKIRT spectrum. But this trend might also be due to a variable continuum level and not necessarily due to changes in the CO emission. To illustrate the real deviations in the emission spectra, we show in Fig. 4 the superposition of the two data sets. For easier comparison, we marked the positions of the band heads and normalized both spectra to the intensity of the first band head. The GNIRS spectrum displays less intensity between the two band heads, which we interpret as due to small differences in the CO column density along with the slightly higher velocity and the different profile shape found for the Pfund lines. The higher the number of the Pfund transition, the closer the wavelengths of the neighbouring lines, leading to strong blending of the lines in the upper transitions of the series and hence to a rise of the total emission.

However, the most striking change in the spectrum is the drastic decrease in the intensity of the (3 ⟶ 1) band head. Because the excitation of the levels within the second band requires considerably higher energies than in the first band, such a vast drop in intensity is a clear indication for a significant decrease in gas temperature. To demonstrate the influence of the temperature on the intensity of the second band had, we show in Fig. 5 the synthetic spectra from CO gas with temperatures of 3500 K (red line) and 1500 K (black line), whereas all other parameters were kept constant. The emission spectra have also been normalized to the intensities in the first band head. The sensitivity of the intensity of the (3 ⟶ 1) band head with temperature is obvious, reinforcing our conclusion that the conditions in the CO forming regions around MWC 349A have changed since 1998.

In this context, it is interesting to note that the first mentioning of CO band emission from MWC 349A was by Geballe & Persson (1987) based on a spectrum taken on 1985 July 1. Despite of the low-resolution ($R \sim 650$), they clearly resolved the first three band heads in their data. CO band emission was already present in a spectrum (though not shown in the paper) taken in 1983 by Hamann & Simon (1986), whereas no indication of CO emission had been seen in the spectra that Thompson & Reed (1976) acquired on 1975 October 13 with an even higher resolution ($R \sim 1000$) compared to the data of Geballe & Persson (1987). Another spectrum with $R \sim 1000$ had been taken on 1997 August 2 displaying CO band emission, also with at least three prominent band heads (Kraus et al. 2000), while in the new data from 2013 basically only the first two band heads are still visible but with noticeable lower intensity.

The absence of detectable CO band emission in the spectra taken in 1975 suggests that considerable changes in the circumstellar conditions of MWC 349A might have taken place between 1975 and 1983, triggering the generation of detectable CO emission.[4] These powering conditions seem now not to be fulfilled any more, resulting in a cooling of the gas and an associated fading of the observable emission.

In light of the fact that MWC 349A is an evolved massive star, a possible scenario for the appearance and fading of the CO band emission might be related to an episode with enhanced mass-loss. In this regard, it is worth mentioning that for MWC 349A a systematic drop in visual brightness has been recorded in the literature during the last century. Starting with a visual magnitude

[4]Changes in the CO band spectrum can also arise from asymmetries or density inhomogeneities within the molecular ring. However, the drastic change in temperature would not fit to such a scenario, unless one postulates a highly eccentric ring of gas. But there is currently no observational evidence that would support such a hypothesis.

of 13.2 mag (Merrill, Humason & Burwell 1932), Swings & Struve (1942) reported that the star was fainter than 14 mag during their observations in 1941, while a value of ∼15.5 mag was obtained 30 yr later by Braes et al. (1972). Recent photometric measurements reveal that the star brightened again to $V = 13$ mag (Manset et al. 2017).

Variability in the red light with a possible period of 9 yr was reported by Jorgenson, Kogan & Strelnitski (2000) based on the analysis of a sample of photometric plates spreading from 1967 to 1981. Moreover, a change in radio continuum appearance from the former bipolar-shaped structure seen in the 1980s into a square-like structure has been found by Rodríguez, Gómez & Tafoya (2007) on new radio images taken in 2004. However, the physical cause of this morphological change is yet unclear. All these pieces provide clear evidence for a variable nature of MWC 349A.

To complement our findings for MWC 349A, we wish to mention that a sudden appearance of CO band emission has also been recorded for the B[e] supergiant LHA 115-S 65 in the Small Magellanic Cloud (Oksala et al. 2012) as well as for the Galactic object CI Cam (Liermann et al. 2014), in which CO emission appeared after an outburst, and faded with the dilution of the ejected material. Other B[e] supergiants were found to display fluctuations in their CO band emission that was ascribed to density inhomogeneities within their circumstellar molecular gas ring. Such a scenario has been proposed for the two B[e] supergiants LHA 120-S 73 (Kraus et al. 2016) and LHA 120-S 35 (Torres et al. 2018) in the Large Magellanic Cloud, and the Galactic B[e] binary object HD 327083 (Kraus et al. 2013a).

5 CONCLUSIONS

We have presented new high-resolution *K*-band spectra for the Galactic emission-line star MWC 349A, based on which we could solve the long-standing issue of the star's unclear nature. The discovery of a significant enrichment of the circumstellar material in ^{13}CO rules out a pre-main sequence nature of the central star, but reinforces the classification of MWC 349A as evolved massive star. Proposed literature classifications are a B[e] supergiant (Hartmann et al. 1980; Hofmann et al. 2002) or a luminous blue variable (Gvaramadze & Menten 2012). Considering its near-IR colours, MWC 349A appears clearly offset from luminous blue variables within the near-IR colour–colour diagram, but shares its location with the B[e] supergiants (Kraus 2019). Therefore, we propose that MWC 349A belongs to the group of B[e] supergiants.

This finding is further supported by the variability in the CO emission spectrum, which seems to be inherent in B[e] supergiants. The clear decrease in CO intensity that we note from comparison of our new spectrum to data taken about 15 yr ago with the same spectral resolution is caused by a significant cooling of the gas from about 3500 K down to 1500 K. In combination with the fact that the brightness of MWC 349A considerably dropped by more than 2 mag between the thirties and the seventies of the last century, and that CO emission only started to appear in the infrared spectra of MWC 349A after 1975, we further propose that the star underwent a phase of enhanced mass-loss or mass ejection providing the environment for efficient molecule formation in order to generate pronounced CO band emission. With the brightening of the star back to its original value, it seems that the ejected material has been expanding and cooling, leading to the observed fading of the CO emission.

Variability in emission and in brightness seems to be an inherent property in this type of evolved massive stars, and a higher observing cadence is worthwhile to unveil the time-scales for the variabilities and their physical origin.

ACKNOWLEDGEMENTS

We thank the anonymous referee for valuable comments on the manuscript. This research made use of the NASA Astrophysics Data System (ADS) and of the SIMBAD data base, operated at CDS, Strasbourg, France. MK acknowledges financial support from the Grant Agency of the Czech Republic (GA ČR, grant no. 17-02337S). The Astronomical Institute Ondřejov is supported by the project RVO:67985815. MLA acknowledges financial support from Universidad Nacional de La Plata (Programa de Incentivos 11/G160). LSC acknowledges financial support from CONICET (PIP 0177) and the Agencia Nacional de Promoción Científica Tecnológica (ANPCyT 2016–1971). This project has received funding from the European Union's Framework Programme for Research and Innovation Horizon 2020 (2014–2020) under the Marie Skłodowska-Curie grant agreement no. 823734.

This study is based on observations obtained at the Gemini Observatory, which is operated by the Association of Universities for Research in Astronomy, Inc., under a cooperative agreement with the NSF on behalf of the Gemini partnership: the National Science Foundation (United States), National Research Council (Canada), CONICYT (Chile), Ministerio de Ciencia, Tecnología e Innovación Productiva (Argentina), Ministério da Ciência, Tecnologia e Inovação (Brazil), and Korea Astronomy and Space Science Institute (Republic of Korea) under programme IDs GN-2013A-Q-78 and GN-2013B-Q-11.

REFERENCES

Altenhoff W. J., Strittmatter P. A., Wendker H. J., 1981, A&A, 93, 48
Andrillat Y., Jaschek M., Jaschek C., 1996, A&AS, 118, 495
Aret A., Kraus M., Šlechta M., 2016, MNRAS, 456, 1424
Braes L. L. E., Habing H. J., Schoenmaker A. A., 1972, Nature, 240, 230
Báez-Rubio A., Martín-Pintado J., 2017, in Miroshnichenko A., Zharikov S., Korčáková D., Wolf W., eds, ASP Conf. Ser. Vol. 508, The B[e] Phenomenon: Forty Years of Studies. Astronomical Society of the Pacific, San Francisco, p. 279
Báez-Rubio A., Martín-Pintado J., Thum C., Planesas P., 2013, A&A, 553, A45
Báez-Rubio A., Martín-Pintado J., Thum C., Planesas P., Torres-Redondo J., 2014, A&A, 571, L4
Carr J. S., 1989, ApJ, 345, 522
Carr J. S., 1995, Ap&SS, 224, 25
Cohen M., Bieging J. H., Dreher J. W., Welch W. J., 1985, ApJ, 292, 249
Danchi W. C., Tuthill P. G., Monnier J. D., 2001, ApJ, 562, 440
Drew P., Strelnitski V., Smith H. A., Mink J., Jorgenson R. A., O'Meara J. M., 2017, ApJ, 851, 136
Ekström S. et al., 2012, A&A, 537, A146
Elias J. H., Joyce R. R., Liang M., Muller G. P., Hileman E. A., George J. R., 2006, Proc. SPIE, 6269, 62694C
Gaia Collaboration et al., 2018, A&A, 616, A1
Geballe T. R., Persson S. E., 1987, ApJ, 312, 297
Geisel S. L., 1970, ApJ, 161, L105
Gvaramadze V. V., Menten K. M., 2012, A&A, 541, A7
Hamann F., Simon M., 1986, ApJ, 311, 909
Hartmann L., Jaffe D., Huchra J. P., 1980, ApJ, 239, 905
Hofmann K.-H., Balega Y., Ikhsanov N. R., Miroshnichenko A. S., Weigelt G., 2002, A&A, 395, 891
Ilee J. D., Oudmaijer R. D., Wheelwright H. E., Pomohaci R., 2018, MNRAS, 477, 3360

Ilee J. D. et al., 2013, MNRAS, 429, 2960
Jorgenson R. A., Kogan L. R., Strelnitski V., 2000, AJ, 119, 3060
Kourniotis M., Kraus M., Arias M. L., Cidale L., Torres A. F., 2018, MNRAS, 480, 3706
Kramida A., Ralchenko Y., Reader J., and NIST ASD Team, 2019, NIST Atomic Spectra Database (ver. 5.7.1), [Online]. Available: https://physics.nist.gov/asd [2020, March 11]. National Institute of Standards and Technology, Gaithersburg, MD
Kraus M., 2009, A&A, 494, 253
Kraus M., 2019, Galaxies, 7, 83
Kraus M., Cidale L. S., Arias M. L., Oksala M. E., Borges Fernandes M., 2014, ApJ, 780, L10
Kraus M., Krügel E., Thum C., Geballe T. R., 2000, A&A, 362, 158
Kraus M., Oksala M. E., Cidale L. S., Arias M. L., Torres A. F., Borges Fernandes M., 2015, ApJ, 800, L20
Kraus M., Oksala M. E., Nickeler D. H., Muratore M. F., Borges Fernandes M., Aret A., Cidale L. S., de Wit W. J., 2013b, A&A, 549, A28
Kraus M. et al., 2013a, in Massive Stars: From alpha to Omega. id. 160
Kraus M. et al., 2016, A&A, 593, A112
Kraus M. et al., 2017, AJ, 154, 186
Leinert C., 1986, A&A, 155, L6
Liermann A., Kraus M., Schnurr O., Fernandes M. B., 2010, MNRAS, 408, L6
Liermann A., Schnurr O., Kraus M., Kreplin A., Arias M. L., Cidale L. S., 2014, MNRAS, 443, 947
Lumsden S. L., Puxley P. J., 1996, MNRAS, 281, 493
Manset N., Miroshnichenko A. S., Zharikov S. V., Kusakin A. V., 2017, in Miroshnichenko A., Zharikov S., Korčáková D., Wolf M., eds, ASP Conf. Ser. Vol. 508, The B[e] Phenomenon: Forty Years of Studies. Astronomical Society of the Pacific, San Francisco, p. 389
Maravelias G., Kraus M., Cidale L. S., Borges Fernandes M., Arias M. L., Curé M., Vasilopoulos G., 2018, MNRAS, 480, 320
Mariotti J. M., Chelli A., Foy R., Lena P., Sibille F., Tchountonov G., 1983, A&A, 120, 237
Martin-Pintado J., Bachiller R., Thum C., Walmsley M., 1989, A&A, 215, L13
Martín-Pintado J., Thum C., Planesas P., Báez-Rubio A., 2011, A&A, 530, L15
McGregor P. J., Hillier D. J., Hyland A. R., 1988b, ApJ, 334, 639
McGregor P. J., Hyland A. R., Hillier D. J., 1988a, ApJ, 324, 1071
McGregor P. J., Hyland A. R., McGinn M. T., 1989, A&A, 223, 237
Merrill P. W., Humason M. L., Burwell C. G., 1932, ApJ, 76, 156
Meyer J. M., Nordsieck K. H., Hoffman J. L., 2002, AJ, 123, 1639
Morris P. W., Eenens P. R. J., Hanson M. M., Conti P. S., Blum R. D., 1996, ApJ, 470, 597
Muratore M. F., Kraus M., Oksala M. E., Arias M. L., Cidale L., Borges Fernandes M., Liermann A., 2015, AJ, 149, 13
Oksala M. E., Kraus M., Arias M. L., Borges Fernandes M., Cidale L., Muratore M. F., Curé M., 2012, MNRAS, 426, L56
Oksala M. E., Kraus M., Cidale L. S., Muratore M. F., Borges Fernandes M., 2013, A&A, 558, A17
Olnon F. M., 1975, A&A, 39, 217
Rodríguez L. F., Gómez Y., Tafoya D., 2007, ApJ, 663, 1083
Strelnitski V., Bieging J. H., Hora J., Smith H. A., Armstrong P., Lagergren K., Walker G., 2013, ApJ, 777, 89
Strelnitski V., Haas M. R., Smith H. A., Erickson E. F., Colgan S. W. J., Hollenbach D. J., 1996, Science, 272, 1459
Swings P., Struve O., 1942, ApJ, 95, 152
Thompson R. I., Reed M. A., 1976, ApJ, 205, L159
Thum C., Martin-Pintado J., Quirrenbach A., Matthews H. E., 1998, A&A, 333, L63
Thum C., Matthews H. E., Harris A. I., Tacconi L. J., Schuster K. F., Martin-Pintado J., 1994b, A&A, 288, L25
Thum C., Matthews H. E., Martin-Pintado J., Serabyn E., Planesas P., Bachiller R., 1994a, A&A, 283, 582
Torres A. F., Cidale L. S., Kraus M., Arias M. L., Barbá R. H., Maravelias G., Borges Fernandes M., 2018, A&A, 612, A113
Wheelwright H. E., de Wit W. J., Weigelt G., Oudmaijer R. D., Ilee J. D., 2012, A&A, 543, A77
Wheelwright H. E., Oudmaijer R. D., de Wit W. J., Hoare M. G., Lumsden S. L., Urquhart J. S., 2010, MNRAS, 408, 1840
White R. L., Becker R. H., 1985, ApJ, 297, 677
Zhang Q., Claus B., Watson L., Moran J., 2017, ApJ, 837, 53

This paper has been typeset from a TEX/LATEX file prepared by the author.